 CMES, vol.2, no.1, pp.15-26, 2001

The Effect of a Rotational Spring on the Global Stability Aspects of the Classical von Mises Model under Step Loading

D. S. Sophianopoulos[1], **G. T. Michaltsos**[2]

Abstract: The present work deals with the global stability aspects of a simple two-degrees-of-freedom autonomous initially imperfect damped model, under step (conservative) loading. The proposed system is an extension of the classical limit point one firstly introduced by von Mises, with the addition of a linear rotational spring. The effect of its properties (stiffness and damping) are fully assessed and under certain combinations of the parameters involved a third possibility of postbuckling dynamic response is revealed. This is associated with a point attractor response on a stable prebuckling fixed point, although dynamic buckling has already occurred, a finding validating new relevant phenomena reported recently in the literature.

keyword: Modeling, dynamic buckling, point attractors, global stability

1 Introduction

Quite often in engineering practice simple models with a few degrees of freedom (DOFs) are used either as a powerful tool for the simulation of actual continuous structures under various types of loading or for the comprehensive study of numerous instability phenomena as well as for the determination of the static and dynamic stability characteristics of all kinds of distinct critical points [Gioncu and Ivan (1984), Thompson and Hunt (1984), Sophianopoulos (1996)]. Especially one and two DOF autonomous undamped/damped systems are of particular interest, since their nonlinear Lagrange equations of motion can be rather easily treated and the resulting local as well as global dynamics may be properly classified and visualized.

A characteristic example of such a system is the well-known 2-DOF arch model introduced by von Mises and analyzed 30 years ago [Croll and Walker (1972)]. Under step conservative loading applied statically at its top this typical limit point model exhibits snap-through buckling, often called "reverse geometry" or "umbrella" instability. The dynamics of the relevant imperfect damped system are associated with a point attractor response in the large, after the initiation of the dynamic buckling mechanism, occurring through the vicinity of a saddle, with negative total potential.

The addition however of a linear vertical translational spring to the above referenced model, under certain combinations of the geometric and other parameters involved, may give birth to new phenomena, since as shown recently [Sophianopoulos (1999), (2000)] a third possibility of dynamic postbuckling response is revealed; this is associated with a point attractor on prebuckling both locally and globally asymptotically stable fixed points, although dynamic buckling has already taken place.

As a physical extension of the works cited above, the present study introduces a new variation of the von Mises model, by adding a linear rotational spring at its top, interconnecting the inclined translational ones and focuses thereafter on the effect of its properties (stiffness c and damping β) on the system's global stability under step constant directional (vertical) conservative loading of infinite duration. Following a straightforward fully nonlinear dynamic analysis it is found that for relatively "high" geometric configurations the potential system dealt with is of a typical limit point nature, with global response similar to that of the parent model regardless of c, if kept within reasonable values. On the contrary, for "low" geometries the increase of c leads to limit point-like static behavior with negative total potential along the physical equilibrium path. In the sequel the dynamic response after dynamic buckling is related to an escaped

[1] Doctor, Research Fellow (corresponding author, email: dimisof@central.ntua.gr), Metal Structures Lab, Department of Civil Engineering, National Technical University of Athens, 42 Patision Str., 106 82 Athens, Greece

[2] Associate Professor, Metal Structures Lab, Department of Civil Engineering, National Technical University of Athens, 42 Patision Str., 106 82 Athens, Greece

motion, which depending on the value of the damping coefficient β is finally attracted by either remote stable equilibria or stable prebuckling fixed points. Thus the pertinent zero total potential criterion and relevant energy based estimates can no longer be applied [Kounadis (1996), (1999)] ant the newly reported third possibility of post-buckling dynamic response, already quoted, is once again revealed, validating the previous studies and casting new light upon the whole scientific subject.

2 Geometric considerations and mathematical formulation

Let us consider the slightly initially imperfect 2-DOF dissipative von Misses model illustrated in Fig.1, with the addition of a linear rotational spring placed at its top, where a concentrated mass m is located. If k_i, c_i $(i=1,2)$ and c, β are the stiffness and damping coefficients of the translational and rotational springs respectively, the system is initially at rest at the deformed configuration AO' B, a position for which all springs are considered unstressed.

At this state, if w_0, u_0 are the initial vertical and horizontal displacement components, the lengths of the model's springs are given by the following expressions:

$$\ell_{10} = \left[(d+u_0)^2 + (h-w_0)^2\right]^{1/2} = \beta_1 \ell \tag{1}$$

$$\ell_{20} = \left[(d-u_0)^2 + (h-w_0)^2\right]^{1/2} = \beta_2 \ell \tag{2}$$

$$\ell_{c0} = \arctan\frac{d+u_0}{h-w_0} + \arctan\frac{d-u_0}{h-w_0} \tag{3}$$

If the system is acted upon by a constant directional (conservative) step loading P, yielding to a new equilibrium position, defined by AO"B, the new lengths of the springs are now equal to:

$$\ell_1 = \left[(d+u)^2 + (h-w)^2\right]^{1/2} \tag{4}$$

$$\ell_2 = \left[(d-u)^2 + (h-w)^2\right]^{1/2} \tag{5}$$

$$\ell_c = \arctan\frac{d+u}{h-w} + \arctan\frac{d-u}{h-w} + \pi\left[1-\mathrm{sgn}\,(w-h)\right] \tag{6}$$

Setting $q_1 = u$, $q_2 = w$ as generalized coordinates, the strongly nonlinear Lagrange equations governing the motion of the system are given by the well known relation

$$\frac{d}{dt}\left\{\frac{\partial K}{\partial \dot{q}_i}\right\} - \frac{\partial K}{\partial q_i} + \frac{\partial V_T}{\partial q_i} + \frac{\partial F}{\partial \dot{q}_i} = 0 \quad (i=1,2) \tag{7}$$

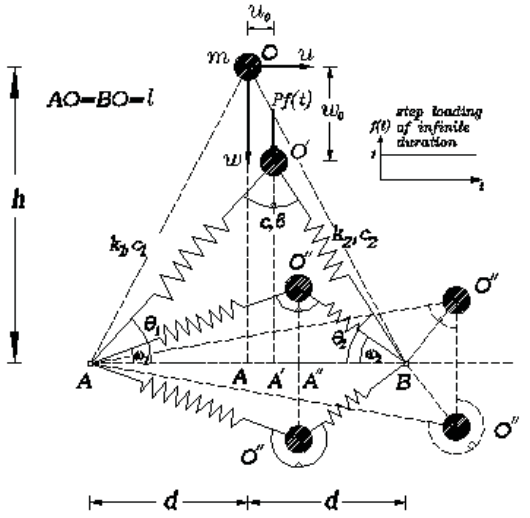

Figure 1 : Geometry and sign convention of the proposed 2-DOF autonomous system

satisfying the following initial conditions

$$q_i = q_{i0} \quad (q_{10} = u_0,\ q_{20} = w_0) \tag{8}$$

$$\dot{q}_i(0) = 0 \quad (i=1,2) \tag{9}$$

In these equations K is the positive definite function of the total kinetic energy, V_T the total potential and F the dissipation function of Rayleigh, while their analytical expressions are

$$K = \frac{1}{2} m\left(\dot{q}_1^2 + \dot{q}_2^2\right) \tag{10}$$

$$V_T = U + \Omega \tag{11}$$

$$F = \frac{1}{2}\sum_{i=1}^{2} c_i \dot{\ell}_i^2 + \frac{1}{2}\beta \dot{\ell}_c^2 \tag{12}$$

where

$$U = \frac{1}{2}\sum_{i=1}^{2} k_i \left(\ell_i - \ell_{0i}\right)^2 + \frac{1}{2} c \left(\ell_c - \ell_{c0}\right)^2 \tag{13}$$

$$\Omega = -P(q_1 - q_{10}) \tag{14}$$

Introducing the dimensionless quantities

$$\tau = \sqrt{\frac{k_1}{m}}t \ \text{(dimensionless time)}, \tag{15}$$

$$\lambda = \frac{P}{k_1 \ell}, \tag{16}$$

$$\overline{\ell}_i = \frac{\ell_1}{\ell} \ (i = 1,2), \tag{17}$$

$$\overline{d} = \frac{d}{\ell}, \tag{18}$$

$$\overline{h} = \frac{h}{\ell} \quad \left(\overline{d}^2 + \overline{h}^2 = 1\right), \tag{19}$$

$$k = \frac{k_2}{k_1}, \tag{20}$$

$$\beta = \frac{\mathbf{\beta}}{\ell^2\sqrt{k_1 m}}, \tag{21}$$

$$\overline{q}_i = \frac{q_i}{l}, \tag{22}$$

$$\overline{q}_{i0} = \frac{q_{i0}}{l}, \tag{23}$$

$$\overline{c}_i = \frac{c_i}{\sqrt{k_1 m}} \quad (i = 1,2), \tag{24}$$

$$\overline{c} = \frac{c}{k_1 \ell^2}. \tag{25}$$

substituting the expressions of the energy functions given in Eq. 10-12 and after cumbersome elaboration, the nonlinear differential equations of motion resulting from Eq. 7 take the following dimensionless form:

$$\begin{aligned}
&\ddot{\overline{q}}_1 + \frac{\partial \overline{V}_T}{\partial \overline{q}_1} + \overline{c}_1 \frac{\overline{d}+\overline{q}_1}{\overline{\ell}_1^2}\left[\left(\overline{d}+\overline{q}_1\right)\dot{\overline{q}}_1 - \left(\overline{h}-\overline{q}_2\right)\dot{\overline{q}}_2\right] + \\
&\quad \overline{c}_2 \frac{\overline{d}-\overline{q}_1}{\overline{\ell}_2^2}\left[\left(\overline{d}-\overline{q}_1\right)\dot{\overline{q}}_1 + \left(\overline{h}-\overline{q}_2\right)\dot{\overline{q}}_2\right] + \\
&\quad \beta\left(\overline{h}-\overline{q}_2\right)\left[\frac{1}{\overline{\ell}_1^2} - \frac{1}{\overline{\ell}_2^2}\right]\left[\frac{\left(\overline{h}-\overline{q}_2\right)\dot{\overline{q}}_1 + \left(\overline{d}+\overline{q}_1\right)\dot{\overline{q}}_2}{\overline{\ell}_1^2} + \right. \\
&\quad \left. \frac{-\left(\overline{h}-\overline{q}_2\right)\dot{\overline{q}}_1 + \left(\overline{d}-\overline{q}_1\right)\dot{\overline{q}}_2}{\overline{\ell}_2^2}\right] = 0
\end{aligned} \tag{26}$$

$$\begin{aligned}
&\ddot{\overline{q}}_2 + \frac{\partial \overline{V}_T}{\partial \overline{q}_2} - \overline{c}_1 \frac{\overline{h}-\overline{q}_2}{\overline{\ell}_1^2}\left[\left(\overline{d}+\overline{q}_1\right)\dot{\overline{q}}_1 - \left(\overline{h}-\overline{q}_2\right)\dot{\overline{q}}_2\right] + \\
&\quad \overline{c}_2 \frac{\overline{h}-\overline{q}_2}{\overline{\ell}_2^2}\left[\left(\overline{d}-\overline{q}_1\right)\dot{\overline{q}}_1 + \left(\overline{h}-\overline{q}_2\right)\dot{\overline{q}}_2\right] + \\
&\quad \beta\left[\frac{\overline{d}+\overline{q}_1}{\overline{\ell}_1^2} - \frac{\overline{d}-\overline{q}_1}{\overline{\ell}_2^2}\right]\left[\frac{\left(\overline{h}-\overline{q}_2\right)\dot{\overline{q}}_1 + \left(\overline{d}+\overline{q}_1\right)\dot{\overline{q}}_2}{\overline{\ell}_1^2} + \right. \\
&\quad \left. \frac{-\left(\overline{h}-\overline{q}_2\right)\dot{\overline{q}}_1 + \left(\overline{d}-\overline{q}_1\right)\dot{\overline{q}}_2}{\overline{\ell}_2^2}\right] = 0
\end{aligned} \tag{27}$$

where

$$\begin{aligned}
\frac{\partial \overline{V}_T}{\partial \overline{q}_1} &= \left[1 - \frac{\beta_1}{\overline{\ell}_1}\right]\left(\overline{d}+\overline{q}_1\right) - k\left[1 - \frac{\beta_2}{\overline{\ell}_2}\right]\left(\overline{d}-\overline{q}_1\right) + \\
&\quad \overline{c}\left(\ell_c - \ell_{c0}\right)\left(\overline{h}-\overline{q}_2\right)\left\{\frac{1}{\overline{l}_1^2} - \frac{1}{\overline{\ell}_2^2}\right\}
\end{aligned} \tag{28}$$

$$\begin{aligned}
\frac{\partial \overline{V}_T}{\partial \overline{q}_2} &= -\left[1 - \frac{\beta_1}{\overline{\ell}_1}\right]\left(\overline{h}-\overline{q}_2\right) - k\left[1 - \frac{\beta_2}{\overline{\ell}_2}\right]\left(\overline{h}-\overline{q}_2\right) + \\
&\quad \overline{c}\left(\ell_c - \ell_{c0}\right)\left[\frac{\overline{d}+\overline{q}_1}{\overline{l}_1^2} + \frac{\overline{d}-\overline{q}_1}{\overline{\ell}_2^2}\right] - \lambda
\end{aligned} \tag{29}$$

subject to initial conditions

$$\overline{q}_i(0) = \overline{q}_{i0}, \quad \dot{\overline{q}}_i(0) = 0 \ \ (i = 1,2) \tag{30}$$

Eliminating the inertia terms from Eqs. 26 and 27 we obtain the necessary and sufficient criterion for static equilibrium that follows

$$\frac{\partial \overline{V}_T}{\partial \overline{q}_1} = \frac{\partial \overline{V}_T}{\partial \overline{q}_2} = 0 \tag{31}$$

with $\overline{V}_T$ being the nondimensionalized total potential energy function.

3 Numerical results and discussion

3.1 Basic assumptions and model cases

For all the model cases dealt with herein we assume that $\overline{q}_{10} = \overline{q}_{20} = 0.01$, while the translational springs are taken identical, i.e. $k = 1$ and $\overline{c}_1 = \overline{c}_2 = 0.05$. Furthermore, two significant model geometries are considered, the first related to "high" systems with $\overline{d} = 0.50$ and the second with "low" ones, for which $\overline{h} = 0.50$. Therefore, two **B**asic **M**odels are use in the subsequent analysis, abbreviated to BM1 and BM2 with the following common properties:

BM1:

$$\overline{q}_{10} = \overline{q}_{20} = 0.01, \quad k = 1, \quad \overline{c}_i = \beta = 0.05, \quad \overline{d} = 0.50$$

BM2:

$$\overline{q}_{10} = \overline{q}_{20} = 0.01, \quad k = 1, \quad \overline{c}_i = 0.05, \quad \overline{h} = 0.50$$

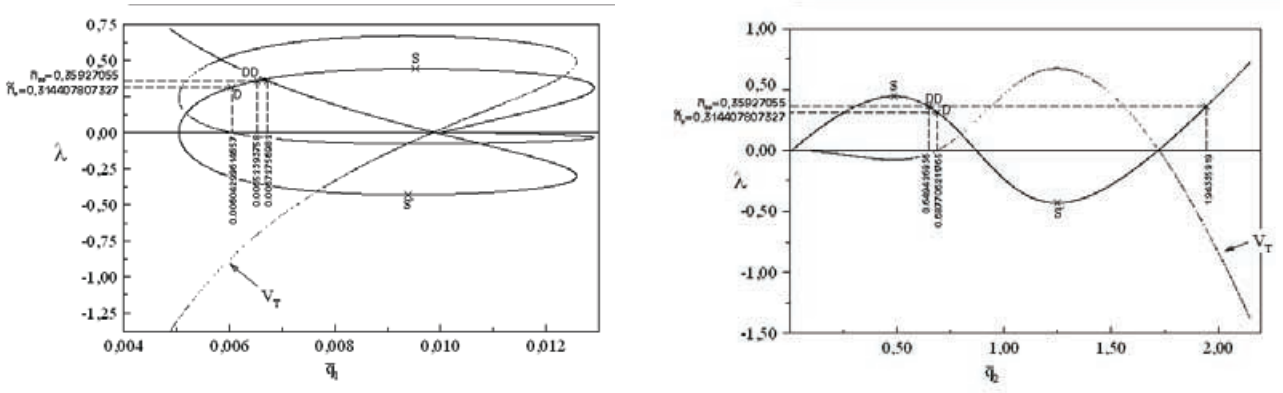

(a) (b)

Figure 2 : Physical equilibrium paths $(\overline{q}_i, \lambda)$ $[i = 1, 2]$ and total potential variation for BM1 with $\overline{c} = 0.001$

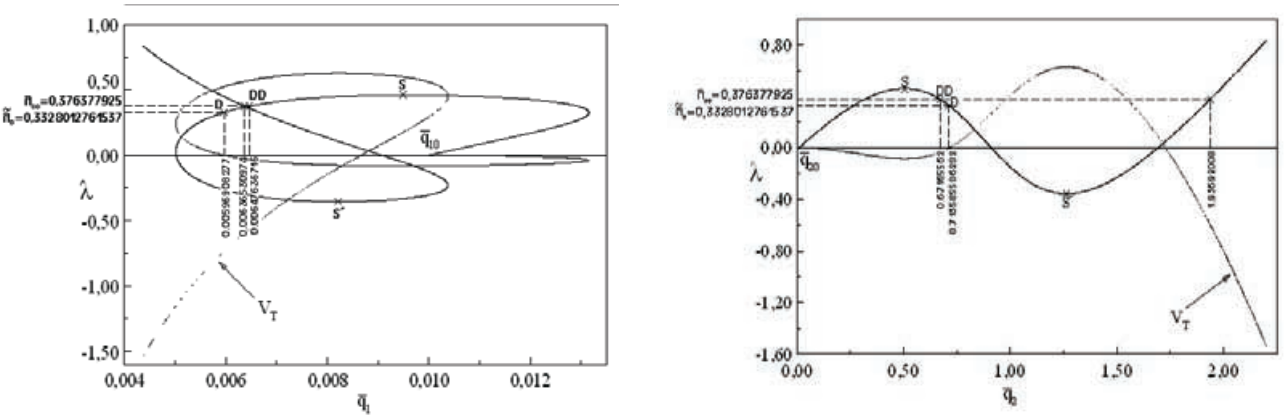

(a) (b)

Figure 3 : Physical equilibrium paths $(\overline{q}_i, \lambda)$ $[i = 1, 2]$ and total potential variation for BM1 with $\overline{c} = 0.01$

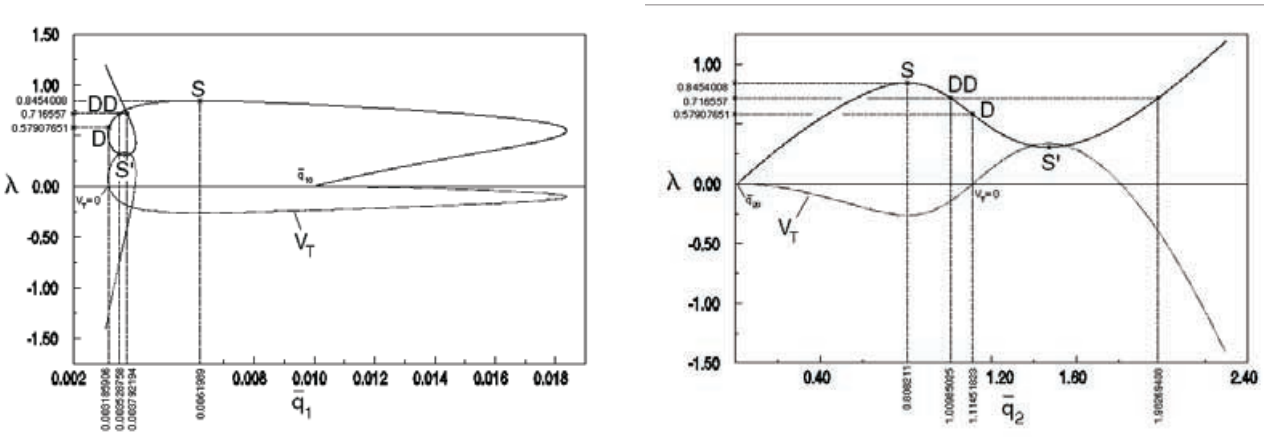

(a) (b)

Figure 4 : Physical equilibrium paths $(\overline{q}_i, \lambda)$ $[i = 1, 2]$ and total potential variation for BM1 with $\overline{c} = 0.1$

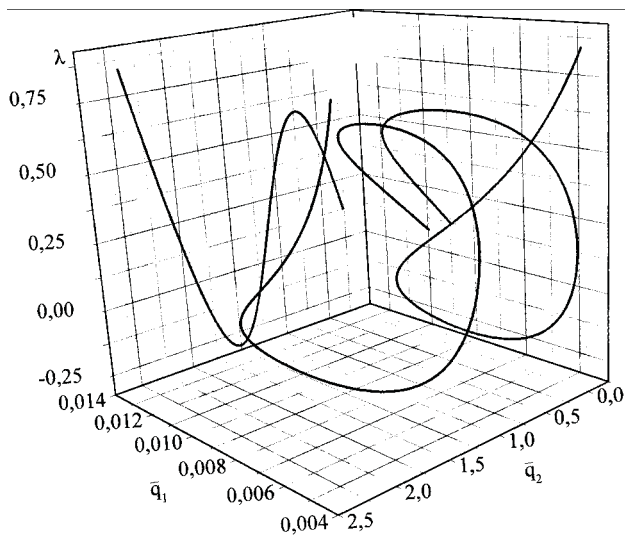

Figure 5 : Physical equilibrium 3D construction for BM1 with $\overline{c} = 0.001$

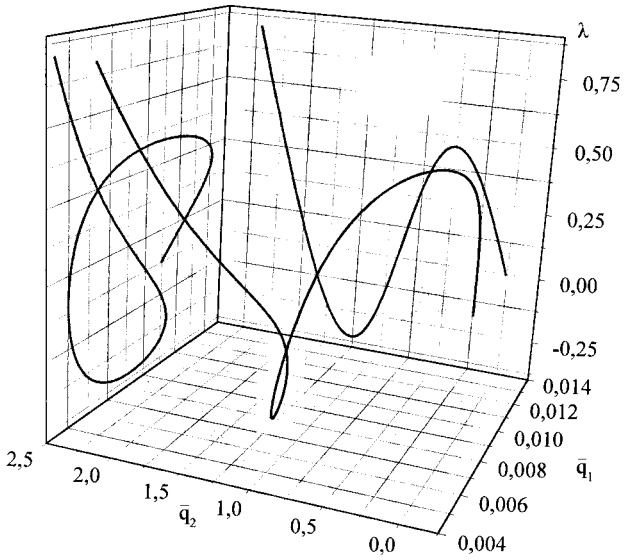

Figure 6 : Physical equilibrium 3D construction for BM1 with $\overline{c} = 0.01$

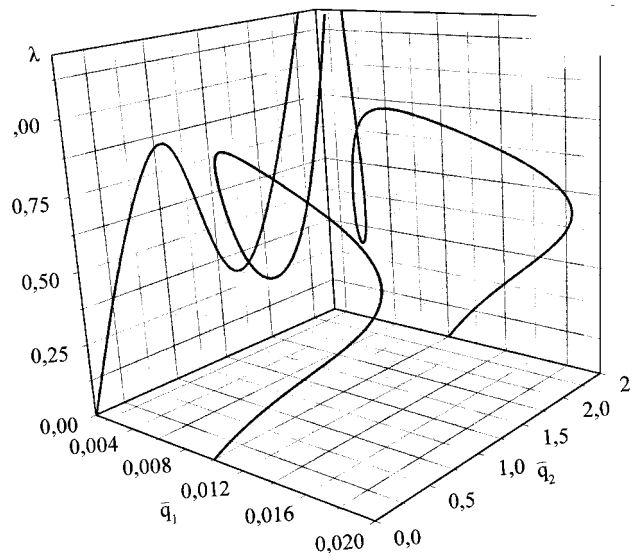

Figure 7 : Physical equilibrium 3D construction for BM1 with $\overline{c} = 0.1$

3.2 Static stability analysis

Solving numerically Eq. 31, by step increasing the value of the vertical displacement $\overline{q}_2$ (which is the dominant one, having the direction of the external loading), with respect to $\overline{q}_1$ and λ, we obtain the staic equilibrium paths $(\overline{q}_i, \lambda)$ for any given set of the foregoing parameters.

*3.2.1 **B**asic **M**odel 1*

For three values of the stiffness $\overline{c}$ of the rotational spring, equal to $c = 0.001$, 0.01 and 0.10 the resulting natural (physical) equilibrium paths are depicted in Figs. 2, 3 and 4 respectively, while their 3D construction throughout Figs.5-7. From these it is evident that the system exhibits a limit point instability associated with snapping, while the variation of $\overline{V}_T$ along these paths is also presented. Thus, the increase of $\overline{c}$ within reasonable values, does not affect the system's static response qualitatively, while its corresponding dynamic one, when damping is accounted for, is associated – as it will be shown below – with a point attractor response in the large, after dynamic buckling. Applying the zero total potential criterion, the values of the approximate dynamic buckling load $\tilde{\lambda}_D$ (for zero damping) is established, being a lower bound of the exact one λ_{DD} valid for the amount of dissipation chose. Notice that the saddle points D and DD are also shown in Figs.2-4, from which it is also perceivable that there are no complementary (physically not accepted) equilibrium configurations, as reported for other 2-DOF systems of similar nature [Sophianopoulos (1999)].

*3.2.2 **B**asic **M**odel 2*

In the same manner as for BM1 and seeking the effect of increasing $\overline{c}$ on the model's response, the physical equilibrium paths for $\overline{c} = 0.001$, 0.01, 0.1 and 1 are established and presented graphically in Figs.8-11, with 3D views depicted in Figs.12-15.

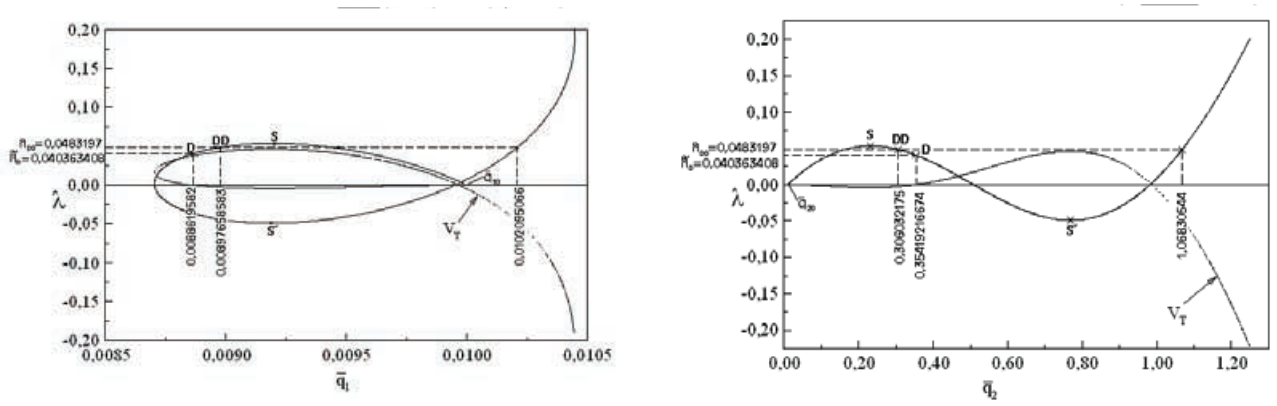

(a) (b)

Figure 8 : Physical equilibrium paths $(\overline{q}_i, \lambda)$ $[i = 1,2]$ and total potential variation for BM2 with $\overline{c} = 0.001$, $\beta = 0.05$

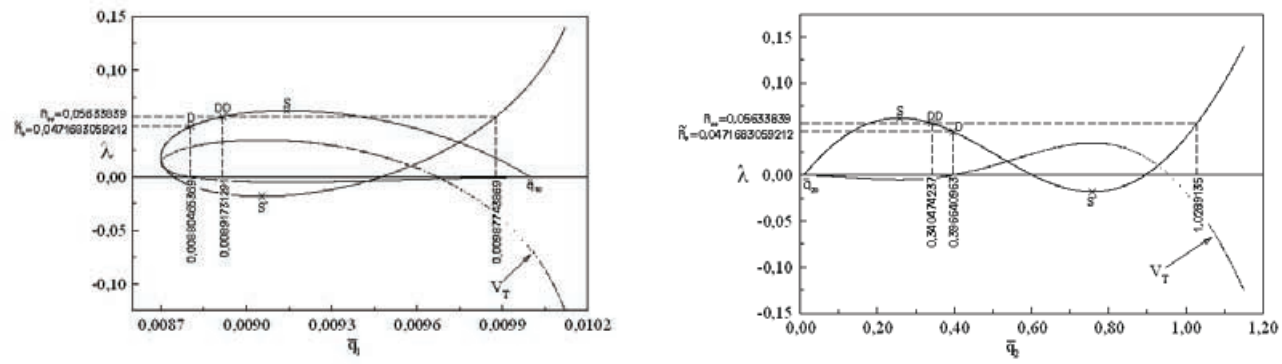

(a) (b)

Figure 9 : Physical equilibrium paths $(\overline{q}_i, \lambda)$ $[i = 1,2]$ and total potential variation for BM2 with $\overline{c} = 0.01$, $\beta = 0.05$

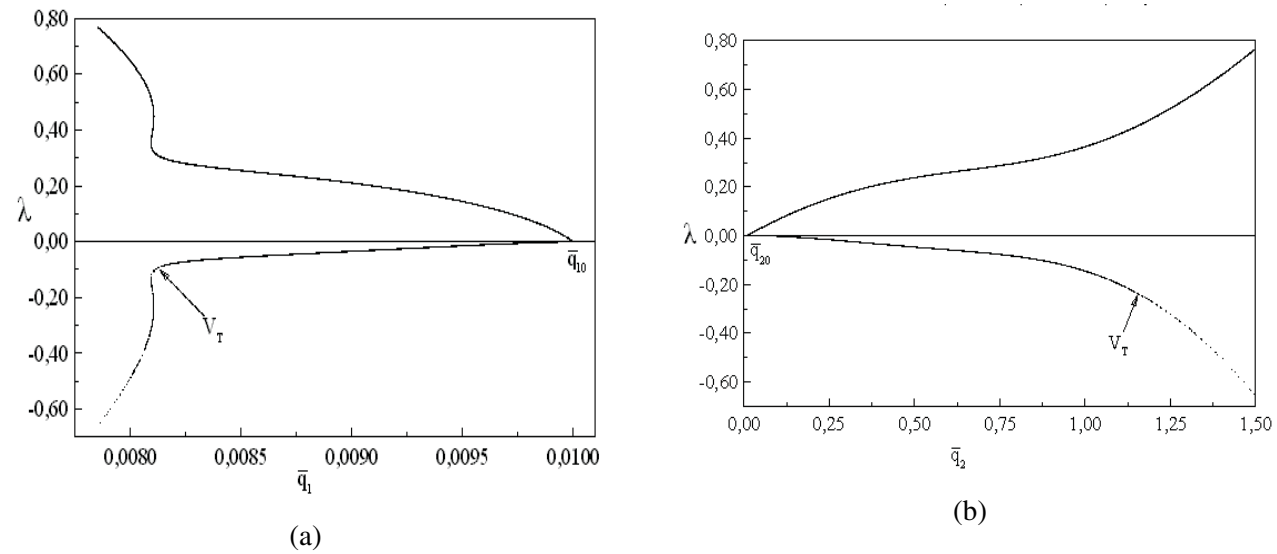

(a) (b)

Figure 10 : Physical equilibrium paths $(\overline{q}_i, \lambda)$ $[i = 1,2]$ and total potential variation for BM2 with $\overline{c} = 0.1$, $\beta = 0.05$

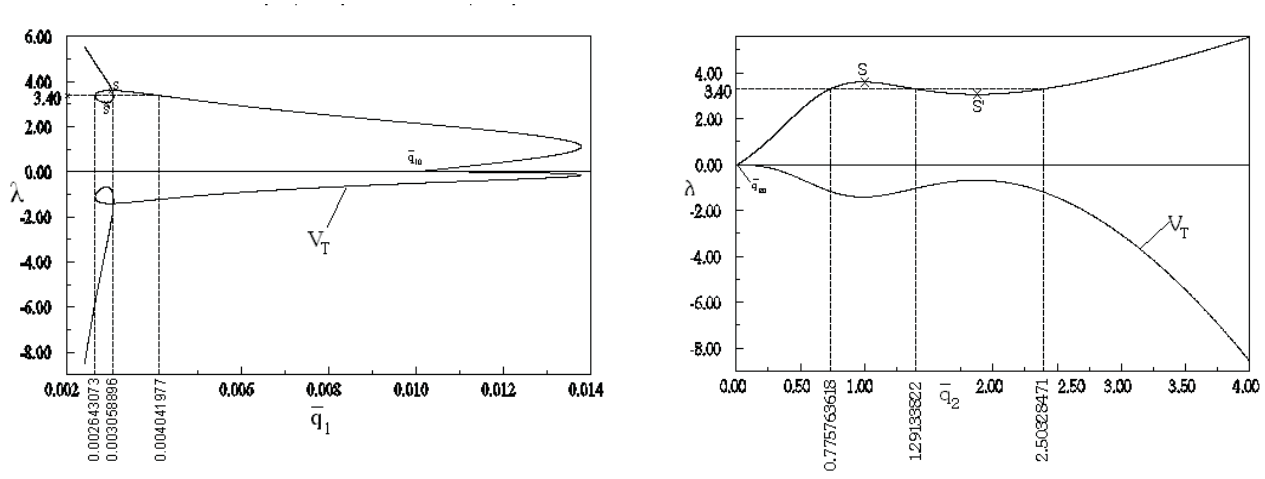

Figure 11 : Physical equilibrium paths $(\overline{q}_i, \lambda)$ $[i = 1,2]$ and total potential variation for BM2 with $\overline{c} = 1$

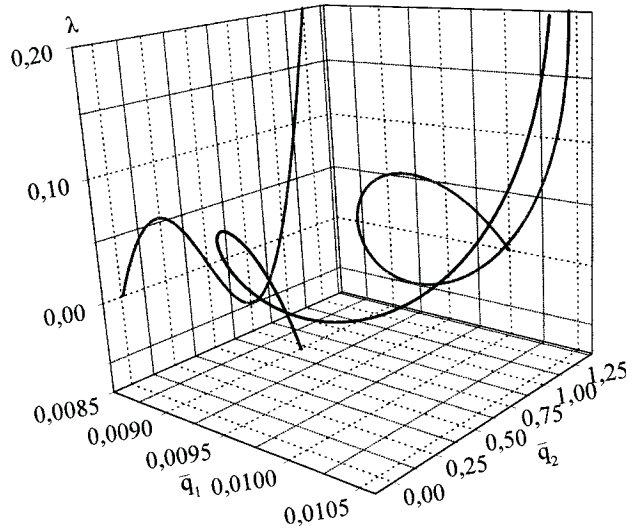

Figure 12 : Physical equilibrium 3D construction for BM2 with $\overline{c} = 0.001$

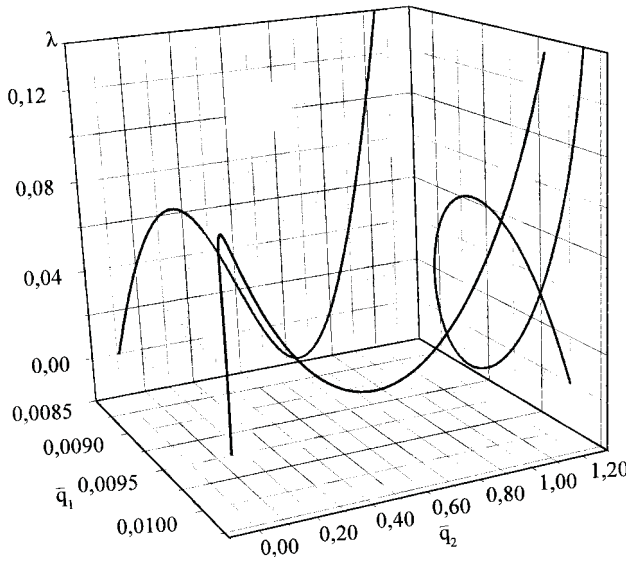

Figure 13 : Physical equilibrium 3D construction for BM2 with $\overline{c} = 0.01$

From these drawings one can directly observe that this "low" model has a significantly smaller load bearing capacity compared to BM1 for the first two values of $\overline{c}$, for which the system is again of a pure limit point nature. Contrary, for $\overline{c} = 0.10$ BM2 exhibits monotonically rising path, implying local and global stability, while the most interesting case is the one associated with $\overline{c} = 1.00$. It is found that this particular model is of a limit point-like nature, since there exist local extremes S and S' (see Fig.11) and simultaneously along the natural path the value of the total potential energy is always negative, a fact implying no restrictions to the corresponding motion [Kounadis, Gantes and Bolotin (1999)]. Between S and S' the fixed points are in fact nonstable saddles [Wiggins

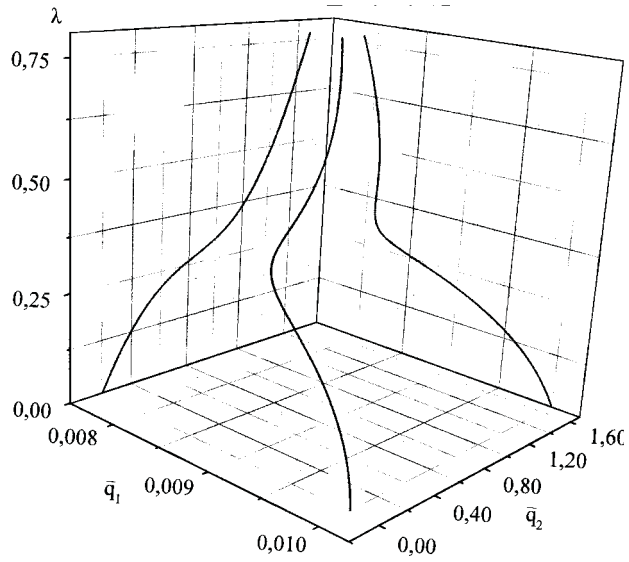

Figure 14 : Physical equilibrium 3D construction for BM2 with $\overline{c} = 0.1$

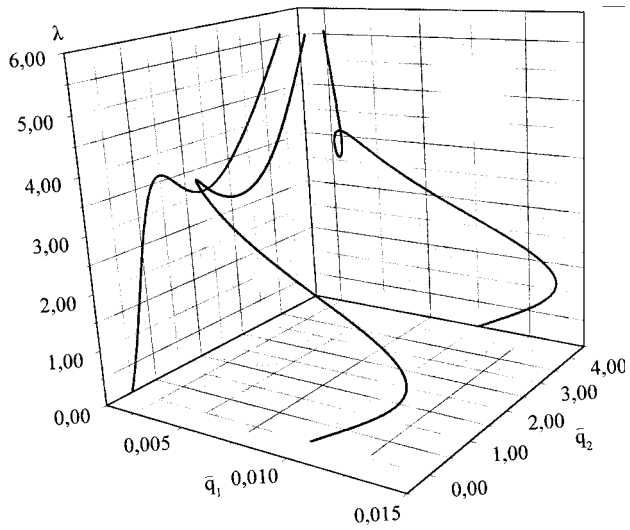

Figure 15 : Physical equilibrium 3D construction for BM2 with $\overline{c} = 1$

(1980)], remaining that way even if the flow is reversed. Thus, the basins of attraction of the pre- and postbuckling stable equilibria corresponding to the same amount of loading $\lambda_{S'} < \lambda < \lambda_S$ are connected to each other forming an escaped passage near the saddles, through which the motion may as well be lead from one domain to the other from both available directions, since there is no repeller barrier. A typical example is shown in the $V_T = 0$ contour and corresponding energy surface representation of Fig.16, for $\lambda = 3.40$. In the sequel the dynamic response should depend on the amount of damping considered, as shown and discussed in a later subsection. The absence of complementary equilibria is a further by-product of the foregoing analysis, as for BM1.

3.3 Dynamic stability analysis

Both basic models, for the cases of limit point instability, exhibit dynamic snap-through occurring in the neighborhood of a saddle DD with negative total potential. The motion thereafter escapes and is attracted by a remote stable fixed point, remaining in its domain and implying global stability. The only difference in the dynamic behavior between the relevant models is that for BM2 the dynamic buckling phenomenon does not happen instantly, but after limited in amplitude and duration oscillations around the saddle. All the above can be observed in the phase plane portraits $[\overline{q}_i(\tau), \dot{\overline{q}}_i(\tau)]$, $i = 1,2$,

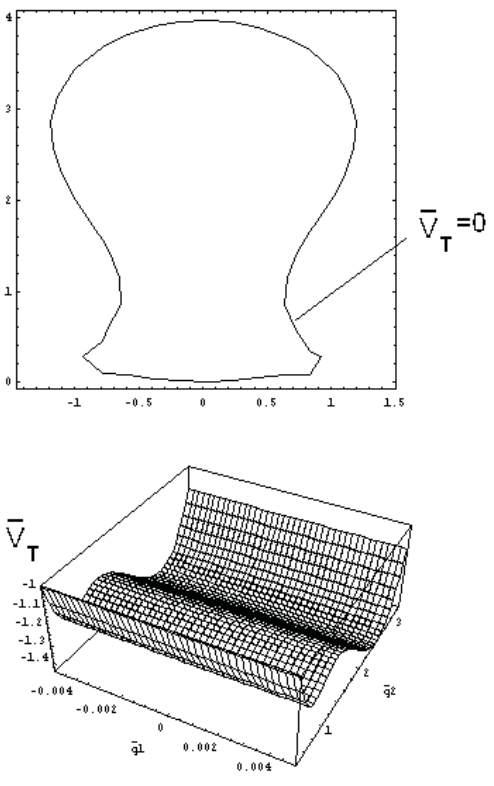

Figure 16 : Contour $\overline{V}_T = 0$ and total potential energy surface of BM2 for $\overline{c} = 1$ and $\lambda = 3.40$

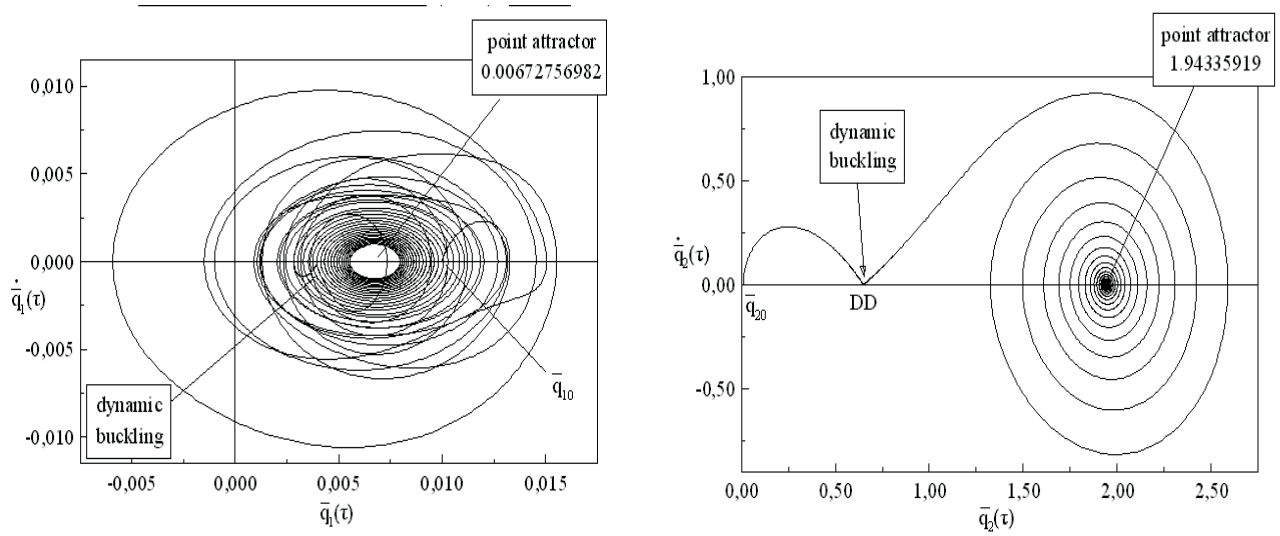

(a) (b)

Figure 17 : Phase plane portraits $[\overline{q}_i(\tau), \dot{\overline{q}}_i(\tau)]$, $(i = 1,2)$ of BM1 for $\overline{c} = 0.001$ at $\lambda = \lambda_{DD} = 0.35927055$

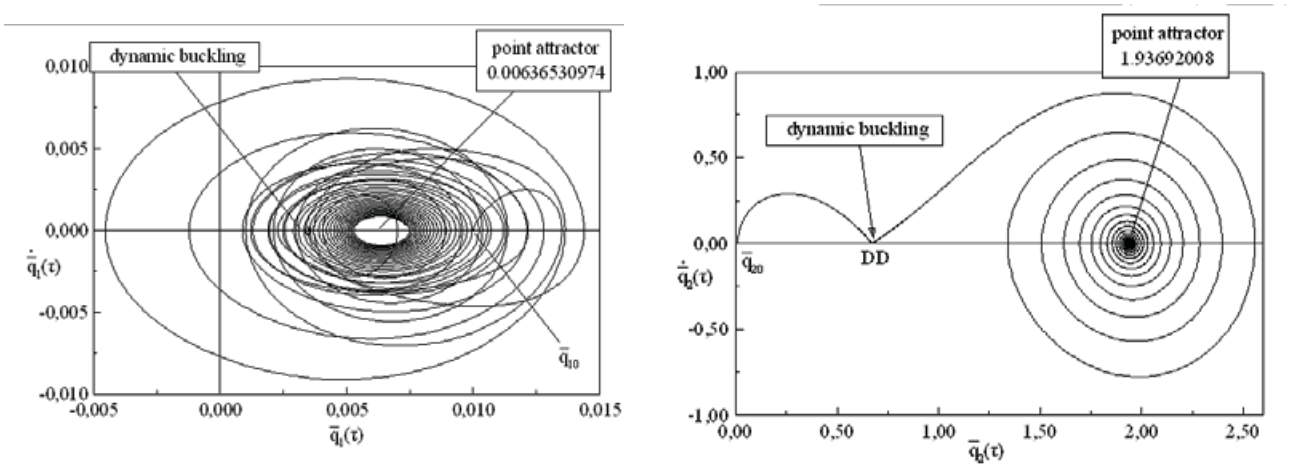

(a) (b)

Figure 18 : Phase plane portraits $[\overline{q}_i(\tau), \dot{\overline{q}}_i(\tau)]$, $(i = 1,2)$ of BM1 for $\overline{c} = 0.01$ at $\lambda = \lambda_{DD} = 0.376377925$

fixed points, a new phenomenon recently reported in the literature.

- Finally, contrary to similar 2-DOF models, the system dealt with does not exhibit complementary physically unacceptable equilibrium configurations.

References

Croll, J. G. A.; Walker, A. C. (1972): *Elements of Structural Stability*. Macmillan Press Ltd.

Gioncu, V.; Ivan, M. (1984): *Theory of critical and postcritical behavior of elastic systems*. Editura Academiei Republicii Socialiste Romania.

Kounadis, A. N. (1993): Static and dynamic, local and global, bifurcations in nonlinear autonomous (damped or undamped) structural systems. *AIAA J.*, vol. 31, no. 8, pp. 1468–1477.

Kounadis, A. N. (1996): Qualitative criteria in nonlinear dynamic buckling and stability of autonomous dissi-

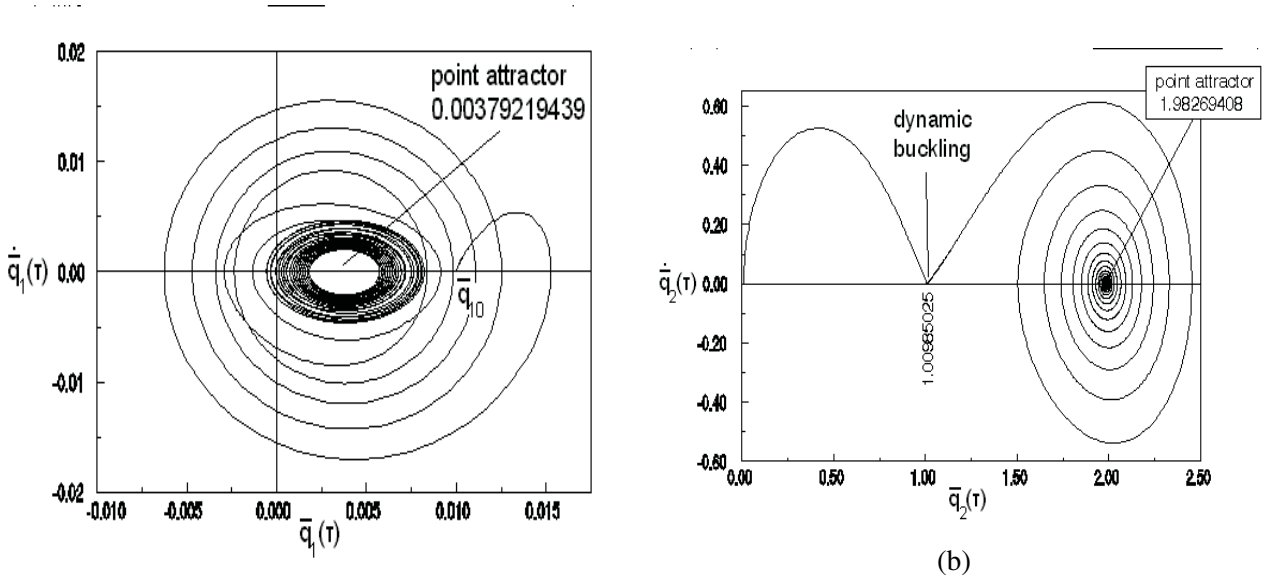

(a) (b)

Figure 19 : Phase plane portraits $[\overline{q}_i(\tau), \dot{\overline{q}}_i(\tau)]$, $(i = 1,2)$ of BM1 for $\overline{c} = 0.1$ at $\lambda = \lambda_{DD} = 0.716557$

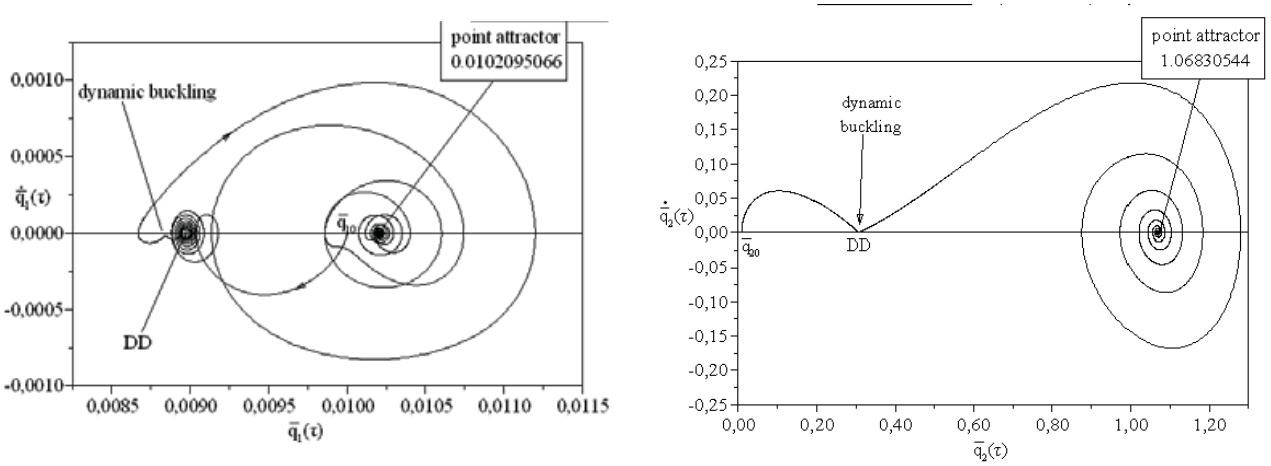

(a) (b)

Figure 20 : Phase plane portraits $[\overline{q}_i(\tau), \dot{\overline{q}}_i(\tau)]$, $(i = 1,2)$ of BM2 for $\overline{c} = 0.001$ at $\lambda = \lambda_{DD} = 0.0483197$

pative systems. *Int. J. Non-Linear Mech.*, vol. 31, pp. 583–612.

Kounadis, A. N. (1999): Geometric approach for establishing dynamic buckling loads of autonomous potential two-degree-of-freedom systems. *J. Appl. Mech.*, vol. 66, no. 1, pp. 55–61.

Kounadis, A. N. (1999): On the nonlinear dynamic buckling mechanism of autonomous dissipative/nondissipative structural systems. *Arch. Appl. Mech.*, vol. 66, no. 6, pp. 395–408.

Kounadis, A. N.; Gantes, C. J.; Bolotin, V. V. (1999): Dynamic buckling loads of autonomous potential systems based on the geometry of the energy surface. *Int. J. Engng Sci.*, vol. 37, no. 12, pp. 1611–1628.

Sophianopoulos, D. S. (1996): Static and dynamic stability of a single-degree-of-freedom autonomous system

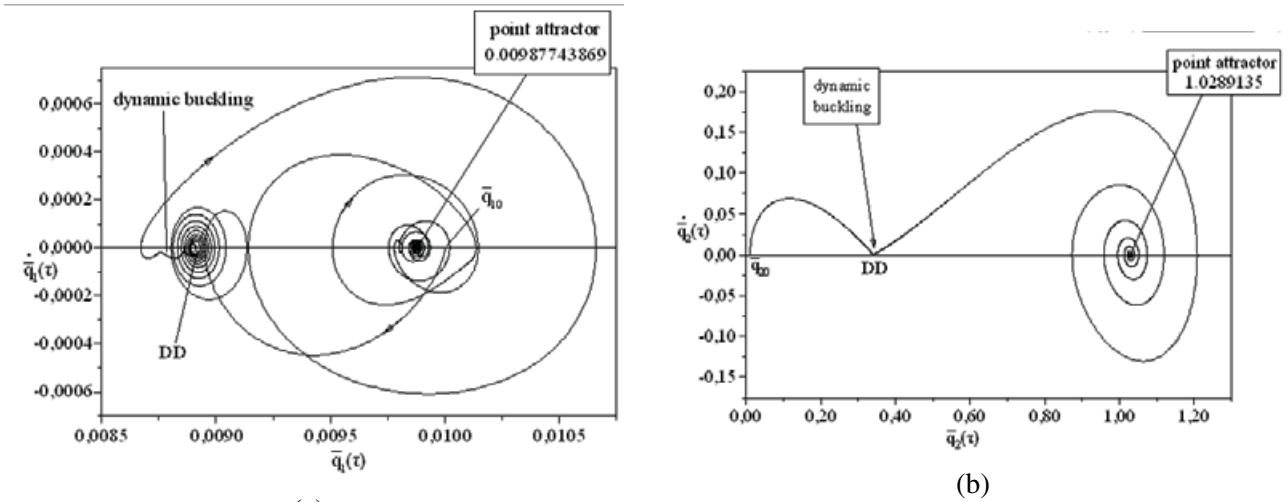

(a) (b)

Figure 21 : Phase plane portraits $[\overline{q}_i(\tau), \dot{\overline{q}}_i(\tau)]$, $(i = 1,2)$ of BM2 for $\overline{c} = 0.01$ at $\lambda = \lambda_{DD} = 0.05633839$

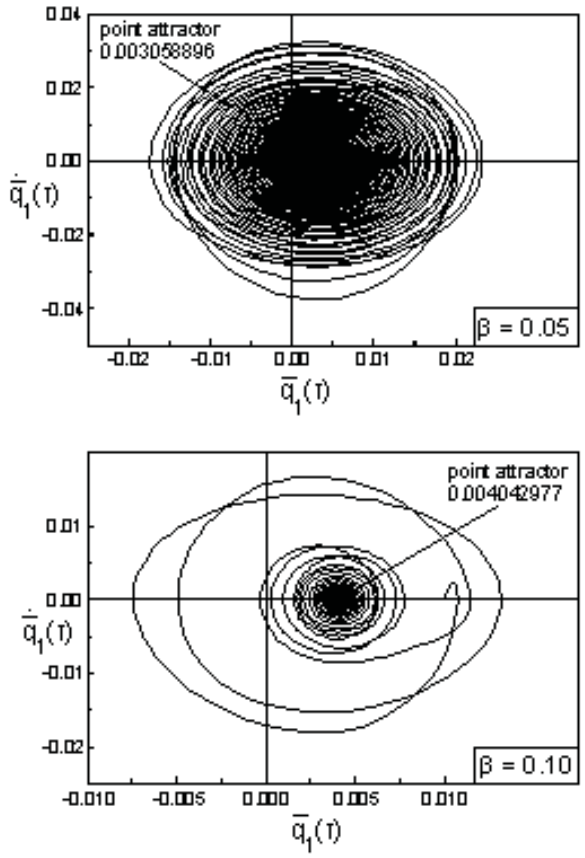

Figure 22 : Phase plane portraits $[\overline{q}_1(\tau), \dot{\overline{q}}_1(\tau)]$ of BM2 for $\overline{c} = 1$ at $\lambda = 3.40$ and two values of damping coefficient $\beta = 0.05, 0.10$

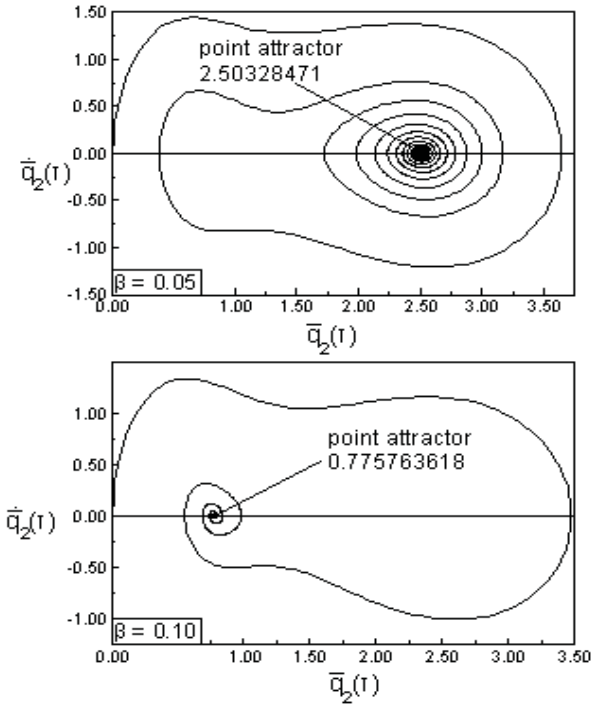

Figure 23 : Phase plane portraits $[\overline{q}_2(\tau), \dot{\overline{q}}_2(\tau)]$ of BM2 for $\overline{c} = 1$ at $\lambda = 3.40$ and two values of damping coefficient $\beta = 0.05, 0.10$

with distinct critical points. *Struct. Engng & Mech.*, vol. 4, pp. 529–540.

Sophianopoulos, D. S. (1999): Point attractors and dynamic buckling of autonomous systems under step loading. *Int. J. Solids Structures*, vol. 36, no. 35, pp. 5357–5385.

Sophianopoulos, D. S. (2000): New phenomena associated with the nonlinear dynamics and stability of autonomous damped systems under various types of loading. *Struct. Engng & Mech.*, vol. 9, no. 4, pp. 397–416.

Sophianopoulos, D. S.; Michaltsos, G. T. (2000): The effect of a rotational spring on the global stability aspects of the classical von mises model under step loading. In Atluri, S. N.; Brust, F. W.(Eds): *Proceedings of the International Conference for Computational Engineering Science (ICES'2K)*, pp. 1846–51, Vol. II, L.A., CA, USA.

Thompson, G. M. T.; Hunt, G. W. (1984): *Elastic instability phenomena*. John Wiley & Sons.

Wiggins, S. (1980): *Introduction to Applied Nonlinear Dynamical Systems and Chaos*. Springer Verlag.